Modeling Coupled Heat and Mass Transfer in Laminar Forced Convection in a Vertical Channel: Influence of the Fluid's Relative Humidity

Ouédraogo Rimnogdo Wilfried[1,2], Bagré Sara[1], Namoano David[2], Igo Wendsida Serge[1]

[1]Centre National de la Recherche Scientifique et Technologique/Institut de Recherche en Sciences Appliquées et Technologies/Laboratoire des Systèmes d'Énergies Renouvelables et Environnement Génie Mécanique Industriel (CNRST/IRSAT/LASERE-GMI), Ouagadougou, Burkina Faso.
[2]Laboratoire d'Energies Thermiques Renouvelables (LETRE), Université Joseph KI-ZERBO, Ouagadougou, Burkina Faso.

Corresponding Author: Ouédraogo Rimnogdo Wilfried

ABSTRACT

The heat and mass exchanges between fluids and walls that accompany two-phase flows in channels are of immeasurable interest in many fields such as energy, food processing, fire engineering, biomedical etc. The aim of the present study is to explore numerically the effect of the relative humidity of an upward laminar forced convection airflow in a channel on heat and mass transfer. The walls of the channel are damp and interact with the outside environment. Based on simplifying assumptions, the flow, whose thermo-physical properties depend on temperature and relative humidity, was modeled by the Navier Stokes equations and the flow conservation equation. The finite volume method was used to discretize the equations, and the resulting systems of algebraic equations were solved using the Thomas and Gauss algorithms. A numerical calculation code written in FORTRAN and validated by comparing our numerical results with those in the literature was used to run the simulations. These numerical simulations, carried out with a relative humidity range of 60 to 90%, a Reynolds number of 500 and a fluid temperature of 323.15K for an ambient temperature of 298.15K, enabled a detailed study of the heat and mass exchanges taking place between fluid and wall. A sensitivity study of the numerical results to the mesh was carried out to demonstrate the stability of the mesh. The numerical results obtained, presented in the form of axial and radial profiles of temperature, mass concentration, Nusselt and Sherwood numbers, reveal the important role of relative fluid humidity in heat and mass transfer in a vertical channel. The heat and mass transfer rates obtained at the leading edge of the channel and at the outlet are different.

Keywords: Heat and mass transfer, relative humidity, Nusselt and Sherwood numbers, vertical channel.

1. INTRODUCTION

Laminar forced convection flows in channels with physical changes of state give rise to highly complex phenomena depending on parameters such as temperature and relative humidity, Reynolds number, etc. In addition to the fundamental aspects of these phenomena, their

applications are many and varied. In addition to the fundamental aspects of these phenomena, their applications are many and varied, e.g. compact heat exchangers, heat preservation of meat products, cooling of electronic components, fire engineering, nuclear reactors and so on. As a result, coupled heat and mass transfer has been the subject of numerous numerical and experimental studies [1-5]. To further explore the influence of hygrothermal and dynamic parameters on flow and transfer, and to demonstrate the importance of taking into account the variability of thermo-physical properties in the mathematical model, Oulaid et al [6], focused on a warm air stream with physical properties taken constant in the first instance, and variable in the second. They revealed a significant discrepancy (between 8% and 30%) between the results of the two models for all hydrodynamic, thermal and mass quantities. Ghrissi et al [7] investigated the influence of air channel entry parameters on heat and mass transfer phenomena within a water-saturated wall. Their aim was to quantify hygrothermal exchanges at the interface between the saturated porous layer and the air blown into the channel, using a mathematical model based on Darcy's model. A hybrid coupling combining both Boltzmann and finite volume methods was proposed. Neglecting interactions with the surrounding environment, they revealed that blowing relatively moist air significantly affected heat and mass exchange at the interface between the porous layer and the channel. On the other hand, blowing relatively dry air dried out the wall. Given the importance of parameters such as temperature, humidity and velocity, some authors have focused on their effects on heat and mass transfer. Boukadida et al [8] investigated the phenomenon of coupled heat and mass transfer by forced convection in a horizontal channel. They looked at the effect of different control parameters on air velocity, temperature and humidity inside the channel. They showed that the air temperature, longitudinal velocity and water vapour concentration increased from the inlet to the outlet of the channel. Also in the case with radiation, the temperature and water vapor concentration at the interface increase. At the end, they presented the effect of different domain control parameters on the Nusselt and Sherwood numbers, with and without radiation. They showed that increasing the air temperature at the channel entrance, in the case with solar radiation, generates an increase in the Nusselt number, whereas the opposite occurs in the case without radiation. The same phenomenon is observed for the Sherwood number. The effect of increasing the concentration of water vapour in the air at the channel entrance has a negative effect on heat transfer, while it improves mass transfer. Du et al [9] studied the heat and mass transfer process of a liquid film in laminar fall along a vertical heated plate with constant heat flux. They revealed that with increasing evaporation rate, the mean temperature decreases and the share of evaporative heat dissipation in the total heat flux increases, demonstrating that evaporation is an important physical factor for heat dissipation when the liquid film flows over a heated plate. Merouani et al [10] carried out a numerical study of condensation by mixed convection of moist air in a vertical channel with non-isothermal walls, taking into account axial diffusion terms, variation in fluid physical properties and film thickness. Their results show that condensation in the presence of non-condensable gases is characterized by a relatively small increase in film thickness. On the other hand, the increase in convective exchanges between the channel wall and the external environment favors condensation and leads to an increase in the heat flux at the wall. Baamrani et al [11] studied the evaporation of a liquid film in a mixed convection flow through a vertical channel where the left wall is subjected to a uniform heat flux density and the right wall is assumed to be insulated and dry. The authors analyzed the effect of heat flux density, liquid inlet temperature and mass flow rate on heat and mass transfer. Their results show that better evaporation of the liquid film is observed for higher heat flux density and liquid inlet temperature or lower mass flow rate. Mechergui [12] has investigated the phenomenon of natural convection evaporation for laminar, two-dimensional, stationary flow in a simple vertical channel. The walls of the channel, on which a film of water of negligible thickness trickles, are subjected to an imposed

temperature or a flow of constant density. The results showed the influence of parameters such as wall temperature, heat flux density, temperature and humidity at the channel inlet on the velocity, concentration and temperature profiles inside the channel, and on heat and matter transfer. Boukadida et al [13] analyzed coupled heat and mass transfer with forced convection evaporation in a horizontal channel. They looked at the phenomenon of water evaporation in a flow of dry air, moist air and superheated steam in an unsteady regime. By monitoring the flow over time, they were able to gain a better understanding of the coupled heat and mass transfer mechanisms involved. Their study showed that the analogy between heat and mass transfer is only valid for low temperatures and low concentrations, where heat transfer by radiation is negligible and the inversion temperature increases with the inlet flow velocity. Helel et al [14] have focused on the mechanisms of heat and mass transfer by laminar or turbulent forced convection with evaporation in a horizontal channel where the bottom wall is assimilated to an unsaturated porous material. In the laminar case, the authors have shown that heat and mass transfers are greater in the vicinity of the leading edge (channel inlet) than towards the outlet. In addition, they presented the effect of injected air temperature and concentration on evaporated water mass. By increasing the temperature of the drying air, the mass of water evaporated increases. The opposite phenomenon is observed for the water vapour concentration of the drying air, until a critical temperature value is reached. In other words, maximum evaporation is observed for more humid drying air. Kassim et al [15] studied the effect of humidity on an ascending air flow accompanied by heat and mass transfer at the entrance to a vertical channel formed by two parallel flat plates, one of which is kept isothermal and humid, and the other adiabatic and dry. A thin film of negligible thickness trickles down the inside face of the wet plate by gravity. The authors show that increasing the humidity of the air at the channel inlet slightly reduces sensible heat transfer and increases latent heat transfer. Turki et al [16] have shown that the contribution of forced convection to heat transfer is greater than that of mixed convection. The results in the literature show that the influence of the inlet fluid's relative humidity on coupled heat and mass transfer in channels has not been sufficiently explored. This parameter plays a vital role in the condensation and evaporation phenomena that accompany fluid flows in various applications. It is clear that an increase in the relative humidity of the fluid at the channel inlet leads to an increase in the relative humidity of the flow. In reality, this variation in humidity is accompanied by complex phenomena that we will investigate through numerical simulations. Our main objective is therefore to study the influence of the relative humidity of the fluid on unsteady flow in forced laminar convection in a vertical channel, where the thermophysical properties of the fluid are not constant but dependent on temperature and humidity.

2. METHODOLOGY
2.1. DESCRIPTION OF THE PHYSICS MODEL
A fluid of temperature T0, velocity U0 and relative humidity ϕ_0 enters a vertical channel. The walls of this channel, of height H, are separated by a distance 2R, R being the radius of the channel. These walls undergo condensation of the water vapour contained in the fluid. Figure 1 shows the physical model of the channel under study.
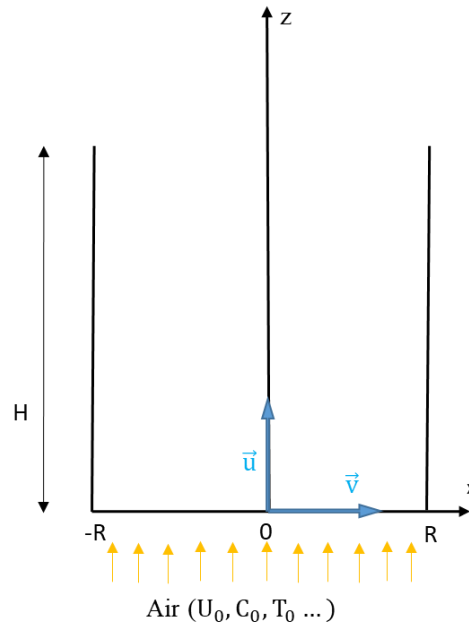
Figure 1. Physical model

2.2. MATHEMATICAL FORMULATION
2.2.1. SIMPLIFYING HYPOTHESES
The hypotheses formulated are:
- The gaseous effluent is laminar, incompressible and Newtonian;
- Transfers are two-dimensional and take place in a forced laminar and unsteady regime;
- The Dufour and Soret effects are neglected;
- The radial driving pressure gradient is neglected;
- The condition of non-slip of the fluid on the walls is considered;
- The flow is rotationally symmetrical around the vertical axis (OZ), which restricts the study on the half channel.

2.2.2. TRANSFER EQUATIONS
In the channel, the equations governing heat and mass transfer, based on the above assumptions, are the Navier-Stokes equations in addition to the flow conservation equation [17-18]. The thermo-physical properties of air are not constant, but depend on temperature and humidity. Their calculation is detailed in the work of Feddaoui et al [19].

❖ **The axial equation of momentum**

$$\rho \frac{\partial U}{\partial t} + \frac{\partial(\rho V U)}{\partial x} + \frac{\partial(\rho U U)}{\partial z} = -\frac{\partial P}{\partial x} + \frac{\partial}{\partial x}\left(\mu \frac{\partial U}{\partial x}\right) + \frac{\partial}{\partial z}\left(\mu \frac{\partial U}{\partial z}\right) \tag{1}$$

❖ **The radial equation of momentum**

$$\rho \frac{\partial V}{\partial t} + \frac{\partial(\rho V V)}{\partial x} + \frac{\partial(\rho U V)}{\partial z} = \frac{\partial}{\partial x}\left(\mu \frac{\partial V}{\partial x}\right) + \frac{\partial}{\partial z}\left(\mu \frac{\partial V}{\partial z}\right) \tag{2}$$

❖ **The continuity equation**

$$\frac{\partial(\rho V)}{\partial x} + \frac{\partial(\rho U)}{\partial z} = 0 \tag{3}$$

❖ **The energy conservation equation**

$$\rho C_p \frac{\partial T}{\partial t} + \frac{\partial(\rho C_p V T)}{\partial x} + \frac{\partial(\rho C_p U T)}{\partial z} = \frac{\partial}{\partial x}\left(\lambda \frac{\partial T}{\partial x}\right) + \frac{\partial}{\partial z}\left(\lambda \frac{\partial T}{\partial z}\right) \tag{4}$$

❖ **The water vapor diffusion equation**

$$\rho \frac{\partial C}{\partial t} + \frac{\partial(\rho VC)}{\partial x} + \frac{\partial(\rho UC)}{\partial z} = \frac{\partial}{\partial x}\left(\rho D \frac{\partial C}{\partial x}\right) + \frac{\partial}{\partial z}\left(\rho D \frac{\partial C}{\partial z}\right) \tag{5}$$

❖ **The flow rate conservation equation**

$$\int_0^R U dx = Q_{ev} + Q_e \tag{6}$$

2.2.3. INITIAL CONDITIONS

$$U(x,z) = 0 \; ; \; V(x,z) = 0 \; ; \; C(x,z) = C_e \; ; \; T(x,z) = T_e \tag{7a-d}$$

2.2.4. BOUNDARY CONDITIONS

- At the channel entrance **: z = 0; 0 ≤ x ≤ R**

$$U(x,z) = \frac{3}{2} U_e \left[1 - \left(\frac{x}{R}\right)^2\right] \tag{8}$$

$$V(x,z) = 0 \; ; \; C(x,z) = C_e \; ; \; T(x,z) = T_e \tag{9a-c}$$

- At the channel outlet : **z = H; 0 ≤ x ≤ R**

$$\frac{\partial U(x,z)}{\partial z} = 0 \; ; \; \frac{\partial V(x,z)}{\partial z} = 0 \; ; \; \frac{\partial T(x,z)}{\partial z} = 0 \; ; \; \frac{\partial C(x,z)}{\partial z} = 0 \tag{10a-d}$$

- At the axis of symmetry: **x = 0; 0 ≤ z ≤ H**

$$V(x,z) = 0 \tag{11}$$

$$\frac{\partial U(x,z)}{\partial x} = 0 \; ; \; \frac{\partial T(x,z)}{\partial x} = 0 \; ; \; \frac{\partial C(x,z)}{\partial x} = 0 \tag{12a-c}$$

- To the wall : **x = R; 0 ≤ z ≤ H**

$$U(x,z) = 0 \tag{13}$$
$$V(x,z) = V_{ev} \tag{14}$$

The detailed calculation of V_{ev} can be found in the work of Eckert et al [20].

$$V_{ev} = -\frac{D}{(1-C_P)} \left.\frac{\partial C}{\partial x}\right|_P \tag{15}$$

The mass fraction of water vapor corresponds to the saturation conditions explained by Dalton's law:

$$C_P = \frac{P_P M_V}{[P_P M_V + (P - P_P) M_a]} \tag{16}$$

$$-\lambda \left(\frac{\partial T}{\partial x}\right) + \rho L_V V_{ev} = -\lambda_s \left(\frac{T_{Pe} - T_{Pi}}{E}\right) = (h_R + h_C)(T_{amb} - T_{Pe}) \tag{17}$$

The convective transfer coefficient h_c is correlated with the Rayleigh number (GrPr) according to J. F Sacadura [21]:

$$h_C = \frac{Nu \lambda_{air}}{H} \tag{18}$$

$$Nu = a(GrPr)^m \tag{19}$$

$$\text{For}: 10^4 < GrPr < 10^9 \; ; \; a = 0.59 \; ; \; m = 0.25 \tag{20}$$

$$\text{For}: 10^9 < GrPr < 10^{13} \; ; \; a = 0.21 \; ; \; m = 0.4 \tag{21}$$

$$Gr = \frac{g\beta_T(T_{Pe} - T_{amb})H^3}{\vartheta_{air}^2} \tag{22}$$

$$h_R = \gamma\sigma\left(T_{Pe}^2 + T_{amb}^2\right)(T_{Pe} + T_{amb}) \tag{23}$$

The total heat flux exchanged between the wet wall and the flow is the sum of the sensible heat flux and the latent heat flux:

$$Q_T = Q_S + Q_L = \lambda\frac{\partial T}{\partial x}\Big|_P + \dot{m}_C'' L_V \tag{24}$$

$$Nu_S = \frac{Dh}{\lambda}\frac{Q_S}{(T_b - T_p)} = \frac{Dh}{(T_b - T_p)}\frac{\partial T}{\partial x}\Big|_P \tag{25}$$

$$Nu_L = \frac{Dh}{\lambda}\frac{Q_L}{(T_b - T_p)} = \frac{\dot{m}_C'' L_V Dh}{\lambda(T_b - T_p)} \tag{26}$$

$$Sh = \frac{Dh}{(C_b - C_p)}\frac{\partial C}{\partial x}\Big|_P \tag{27}$$

$$Re = \frac{UeDh}{\vartheta e} \tag{28}$$

$$Dh = 2R \tag{29}$$

$$Pr = \frac{\rho_e\vartheta_e C_{Pe}}{\lambda_e} \tag{30}$$

$$Sc = \frac{\vartheta_e}{D_e} \tag{31}$$

2.2.5. DIMENSIONLESS EQUATIONS

The dimensionless equations and boundary conditions are obtained by dividing the various variables by the variables by the characteristic quantities of the system given in Table 1.

Table.1. Dimensionless variables

Designation	Dimensionless variable
Radial coordinate	$x^\star = \dfrac{x}{Dh}$
Axial coordinate	$z^\star = \dfrac{z}{Dh}$
Radial velocity	$V^\star = \dfrac{V}{U_e}$
Axial velocity	$U^\star = \dfrac{U}{U_e}$
Temperature	$T^\star = \dfrac{T}{T_e}$
Pressure	$P^\star = \dfrac{P}{\rho_e U_e^2}$
Concentration	$C^\star = \dfrac{C}{C_e}$
Density	$\rho^\star = \dfrac{\rho}{\rho_e}$
Dynamic viscosity	$\vartheta^\star = \dfrac{\vartheta}{\vartheta_e}$

Thermal conductivity	$\lambda^\star = \dfrac{\lambda}{\lambda_e}$
Thermal diffusivity	$D^\star = \dfrac{D}{D_e}$
Specific heat	$Cp^\star = \dfrac{Cp}{Cp_e}$
Radius of channel	$R^\star = \dfrac{R}{Dh}$
Height of channel	$H^\star = \dfrac{H}{Dh}$
kinematic viscosity	$\mu^\star = \dfrac{\mu}{\mu_e}$

❖ **The axial equation of momentum**

$$\rho^* \frac{\partial U^*}{\partial \tau} + \frac{\partial(\rho^* V^* U^*)}{\partial x^*} + \frac{\partial(\rho^* U^* U^*)}{\partial z^*} = -\frac{\partial P^*}{\partial z^*} + \frac{\partial}{\partial x^*}\left(\frac{\mu^*}{Re}\frac{\partial U^*}{\partial x^*}\right) + \frac{\partial}{\partial z^*}\left(\frac{\mu^*}{Re}\frac{\partial U^*}{\partial z^*}\right) \qquad (32)$$

❖ **The radial equation of momentum**

$$\rho^* \frac{\partial V^*}{\partial \tau} + \frac{\partial(\rho^* V^* V^*)}{\partial x^*} + \frac{\partial(\rho^* U^* V^*)}{\partial z^*} = \frac{\partial}{\partial x^*}\left(\frac{\mu^*}{Re}\frac{\partial V^*}{\partial x^*}\right) + \frac{\partial}{\partial z^*}\left(\frac{\mu^*}{Re}\frac{\partial V^*}{\partial z^*}\right) \qquad (33)$$

❖ **The continuity equation**

$$\frac{\partial(\rho^* V^*)}{\partial x^*} + \frac{\partial(\rho^* U^*)}{\partial z^*} = 0 \qquad (34)$$

❖ **The energy conservation equation**

$$\rho^* C_P^* \frac{\partial T^*}{\partial \tau} + \frac{\partial(\rho^* C_P^* V^* T^*)}{\partial x^*} + \frac{\partial(\rho^* C_P^* U^* T^*)}{\partial z^*} = \frac{1}{PrRe}\left[\frac{\partial}{\partial x^*}\left(\lambda^* \frac{\partial T^*}{\partial x^*}\right) + \frac{\partial}{\partial z^*}\left(\lambda^* \frac{\partial T^*}{\partial z^*}\right)\right] \qquad (35)$$

❖ **The water vapor diffusion equation**

$$\rho^* \frac{\partial C^*}{\partial \tau} + \frac{\partial(\rho^* V^* C^*)}{\partial x^*} + \frac{\partial(\rho^* U^* C^*)}{\partial z^*} = \frac{1}{ScRe}\left[\frac{\partial}{\partial x^*}\left(\rho^* D^* \frac{\partial C^*}{\partial x^*}\right) + \frac{\partial}{\partial z^*}\left(\rho^* D^* \frac{\partial C^*}{\partial z^*}\right)\right] \qquad (36)$$

❖ **The flow rate conservation equation**

$$\int_0^{R^*} U^* dx^* = Q_{ev}^* + Q_e^* \qquad (37)$$

2.2.6. INITIAL CONDITIONS

$$U^*(x^*, z^*) = 0 \; ; \; V^*(x^*, z^*) = 0 \; ; \; T^*(x^*, z^*) = 1 \; ; \; C^*(x^*, z^*) = 1 \qquad (38a\text{-}d)$$

2.2.7. BOUNDARY CONDITIONS

▪ At the channel entrance : **z* = 0; 0 ≤ x* ≤ R***

$$U^*(x^*, z^*) = \frac{3}{2}\left[1 - \left(\frac{x^*}{R^*}\right)^2\right] \qquad (39)$$

$$V^*(x^*, z^*) = 0 \; ; \; T^*(x^*, z^*) = 1 \; ; \; C^*(x^*, z^*) = 1 \qquad (40a\text{-}c)$$

▪ To the wall **: x* = R*; 0 ≤ z* ≤ H***

$$U^*(x^*, z^*) = 0 \; ; \; V^*(x^*, z^*) = V_{ev}^* \qquad (41a\text{-}b)$$

$$V_{ev}^* = -\frac{D}{DhU_e\left(1/C_e - C_p^*\right)}\frac{\partial C^*}{\partial x^*}\bigg|_P \tag{42}$$

$$C_p^* = \frac{P_P^* - M_v^*}{P_P^* M_v^* + (P^* - P_P^*)M_a^*} \tag{43}$$

$$\lambda^*\left(\frac{\partial T^*}{\partial x^*}\right) + \frac{\rho^* L_V V_{ev} Dh}{\lambda_e T_e} = \lambda_S^*\left(\frac{T_{Pi}^* - T_{Pe}^*}{E^*}\right) = \frac{Dh}{\lambda_0}(h_R + h_C)(T_{Pe}^* - T_{amb}^*) \tag{44}$$

- At the axis of symmetry: **x* = 0; 0 ≤ z* ≤ H***

$$\partial V^*(x^*, z^*) = 0 \tag{45}$$

$$\frac{\partial U^*(x^*, z^*)}{\partial x^*} = 0 \; ; \; \frac{\partial T^*(x^*, z^*)}{\partial x^*} = 0 \; ; \; \frac{\partial C^*(x^*, z^*)}{\partial x^*} = 0 \tag{46a-c}$$

- At the channel outlet: **z* = H*; 0 ≤ x* ≤ R***

$$\frac{\partial U^*(x^*, z^*)}{\partial z^*} = 0 \; ; \; \frac{\partial U^*(x^*, z^*)}{\partial z^*} = 0 \; ; \; \frac{\partial T^*(x^*, z^*)}{\partial z^*} = 0 \; ; \; \frac{\partial C^*(x^*, z^*)}{\partial z^*} = 0 \tag{47a-d}$$

The Nusselt and Sherwood numbers become:

$$Nu_S = \frac{1}{(T_b^* - T_p^*)}\frac{\partial T^*}{\partial x^*}\bigg|_p \tag{48}$$

$$Nu_L = \frac{\dot{m}_C'' L_V Dh}{\lambda_e \lambda^* T_e (T_b^* - T_p^*)} \tag{49}$$

$$Sh = \frac{1}{(C_b^* - C_p^*)}\frac{\partial C^*}{\partial x^*}\bigg|_p \tag{50}$$

2.3 NUMERICAL METHODOLOGY

The discretization of equations (32), (34), (35) and (36) by the finite volume method [17] leads to an algebraic equation system of N equations with N unknowns. Each equation system obtained is tri-diagonal and is therefore solved by Thomas' algorithm. As for equation (33), it leads to a system of N equations with (N+1) unknowns. For this, it is completed by equation (37) and then solved by the Gauss algorithm. The convergence criterion chosen is:

$$\frac{\phi^{k+1}(I,J) + \phi^k(I,J)}{\phi^{k+1}(I,J)} < 10^{-5} \tag{51}$$

Where k represents the number of iterations and ϕ = T*, C*, U*, V*.

3. RESULTS AND DISCUSSION

The results are recorded when the regime stabilizes at a time t = 3500s and are presented in tabular, profile and iso-values form under the following conditions: T_{amb}=298.15K, T_e=323.15K with Reynolds number equal to 500.

3.1. MODEL VALIDATION

To validate our numerical calculation code, we compared our numerical results with those of Othmane [22], for a stationary flow with channel inlet temperature T0 = 20°C, humidity 50%, Reynolds number 400, Prandtl and Schmidt numbers 0.703 and 0.592 respectively. The

channel walls are maintained at a temperature of 40°C. The results obtained for the sensitive Nusselt number are shown in the figure.2. The relative error resulting from comparison of the two results is of the order of 7%.
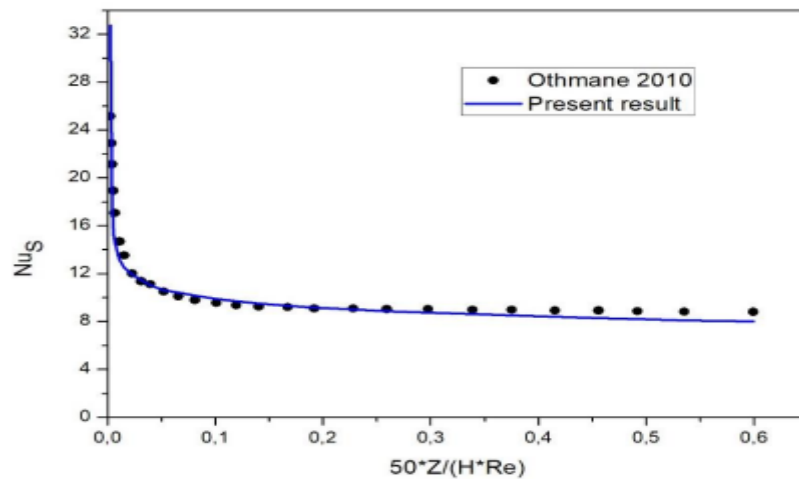

Figure 2: Validation of the numerical code (To = 20°C, Tw = 40°C, ϕ_o = 50%, Pr = 0.703, Sc = 0.592, Re = 400)

3.2. MESH SENSITIVITY STUDY

To ensure that our results are independent of the mesh, a mesh sensitivity study was carried out. This study showed that the mesh size (41x112), even quadrupled, did not significantly modify the sensitive Nusselt (see Table 2). Consequently, the mesh (41x112) was retained for the rest of the study.

Table.2. Grid independence

Grid (X*, Z*)	Z*=20	Z*=40	Z*=60	Z*=80
Values of NuS				
(41x112)	8,0186	6,5718	5,9367	5,5652
(82x224)	8,7732	6,8555	5,9899	5,4705

3.3. INFLUENCE OF RELATIVE FLUID HUMIDITY ON RADIAL TEMPERATURE AND MASS FRACTION PROFILES

Figures 3 and 4 illustrate the radial evolution of the mean fluid temperature and mass fraction at a point Z located halfway up the channel, as a function of the relative humidity of the fluid at the channel inlet, for a constant Reynolds number of 500 and an ambient temperature of 298.15K.
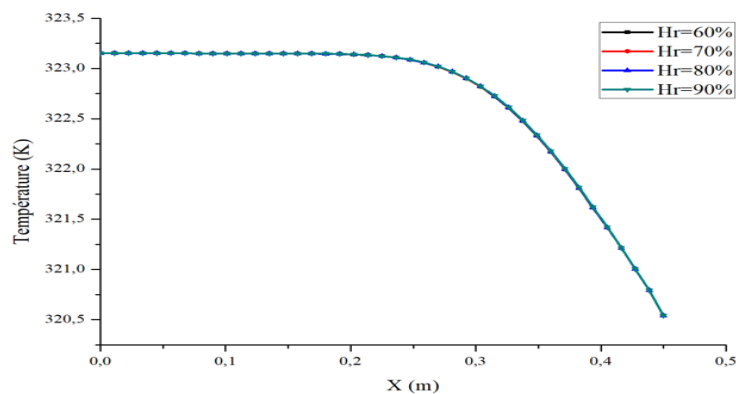

Figure 3. Evolution of the temperature at mid-channel height as a function of the relative humidity of the fluid at the channel inlet
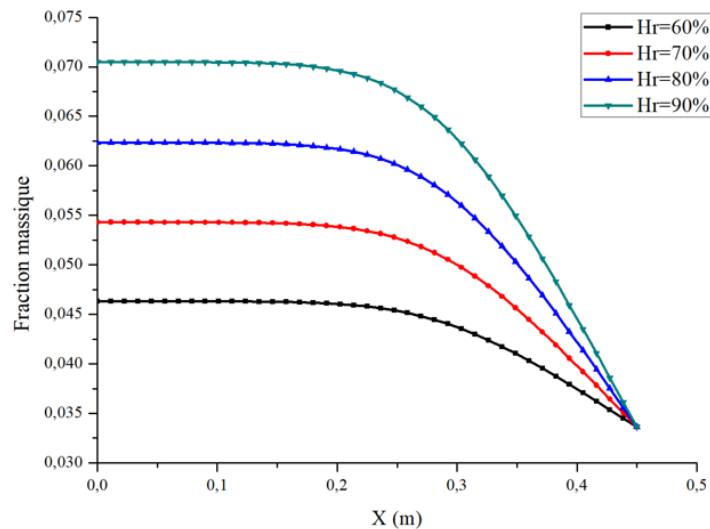
Figure 4. Evolution of the mass concentration at mid-channel height as a function of the relative humidity of the fluid at the channel inlet

The profiles reveal a lesser influence of the fluid's relative humidity on temperature. On the other hand, the influence on mass concentration at the same Z coordinate is clearly significant. We see a gradual increase in the mass concentration of water vapour in the fluid as a function of increasing relative humidity at the inlet. This result seems trivial, since the mass concentration of water vapour in the fluid is intimately linked to relative humidity.

3.4. INFLUENCE OF RELATIVE HUMIDITY ON SENSITIVE AND LATENT NUSSELT NUMBERS

Figures 5 and 6 show the evolution of the latent and sensitive Nusselt numbers along the channel as a function of the relative humidity of the inlet fluid.
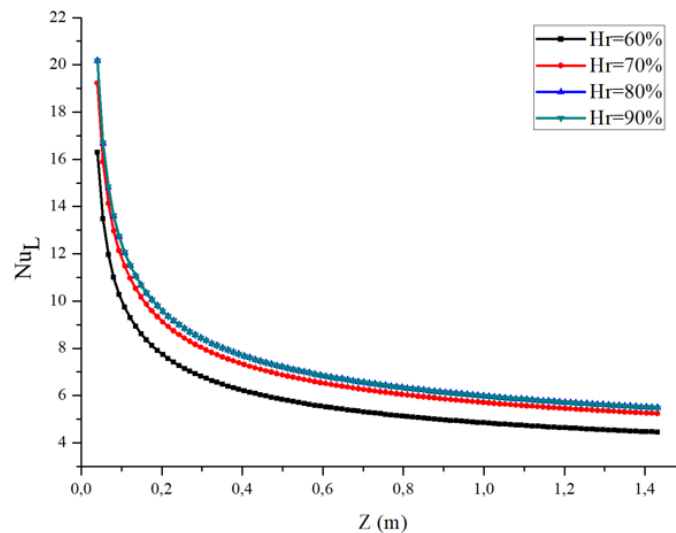

Figure 5. Evolution of the local latent Nusselt number along the channel as a function of the relative humidity of the fluid at the channel inlet
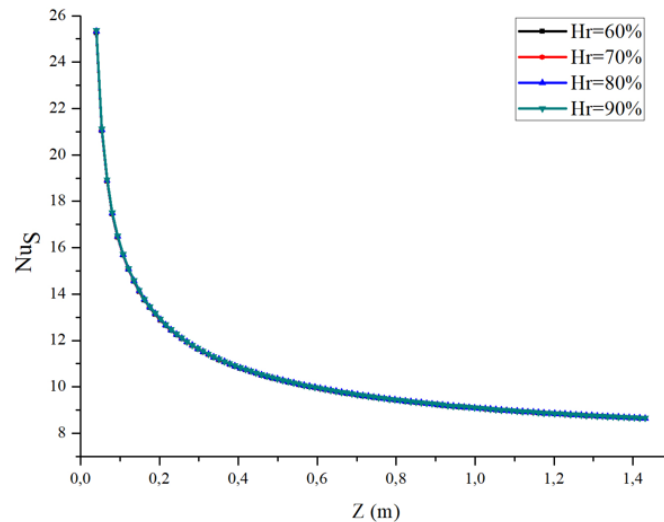
Figure 6. Evolution of the sensitive Nusselt number along the channel as a function of the relative humidity of the fluid at the channel inlet

The latent Nusselt number and sensitive Nusselt number profiles show significant values at the leading edge of the channel. These values decrease along the length of the channel. We note that as the relative humidity of the fluid at the channel entrance increases, heat transport by the latent mode increases, while that by the sensible mode remains more or less constant. At the leading edge of the channel, mass and thermal gradients are significant. They generate large latent and sensible Nusselt numbers, which diminish as the fluid moves through the channel. As the wall is less humid than the fluid, any increase in the relative humidity of the fluid increases the mass gradient between the fluid and the wall. As the relative humidity of the fluid increases, water vapour condenses on the wall. As this condensation is an exothermic reaction, it enhances sensible heat transfer. This improvement is attenuated by the cooling of the fluid due to the increase in its relative humidity.

3.5. INFLUENCE OF RELATIVE HUMIDITY ON SHERWOOD NUMBER
Figure 7 shows the evolution of the Sherwood number under the influence of the relative humidity of the fluid at the channel inlet.
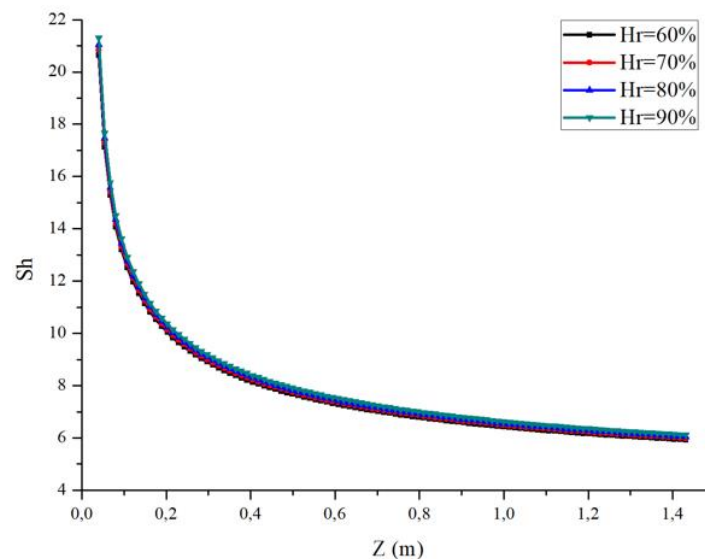

Figure 7. Evolution of the local Sherwood number along the channel as a function of the relative humidity of the fluid at the channel inlet

Like Nusselt numbers, Sherwood numbers exhibit strong gradients at the channel inlet, tending towards a critical value at the channel outlet. An increase in the Sherwood number is observed as the relative humidity of the fluid at the inlet increases. In fact, increasing relative humidity has a considerable influence on the mass fraction of steam in the flow and therefore on mass transfer with the wall. The higher the humidity of the fluid, the greater the condensation. The amount of heat released by this process attenuates the drop in fluid temperature caused by the cooling effect of rising humidity.

CONCLUSION

In the present work, we have carried out a numerical study of coupled heat and mass transfer in a vertical channel whose heat exchange with the outside environment is governed by natural convection and radiation. Forced laminar flow was modeled by the Navier-Stokes equations and the flow conservation equation. These equations were discretized using the finite volume method and then solved using the Thomas and Gauss algorithms. The influence of the relative humidity of the fluid at the channel inlet on heat and mass transfer was a particular focus of attention. A numerical simulation was carried out with a fluid flow of inlet temperature 323.15K, under a Reynolds number of 500 with an ambient temperature of 298.15K. The thermo-physical properties of the fluid are dependent on temperature and humidity. Our numerical results indicate that an increase in the relative humidity of the fluid at the channel inlet leads to an increase in latent-mode mass and heat transfer. This high humidity leads to condensation of the water vapour contained in the fluid, an exothermic process that attenuates the cooling of the flow.

REFERENCES
1. O. R. Wilfried, I. W. Serge, O. Ousmane et al. Modeling heat and mass transfer in laminar forced convection in a vertical channel: Influence of Reynolds number. Physical Science International Joural. 2024; 28(5):48–61, 2024, DOI:10.9734/psij/2024/v28i5847.
2. A. I. Alsabery, N. A. C. Sidik, I. Hashim et al. Impacts of two-phase nanofluid approach toward forced convection heat transfer within a 3D wavy horizontal channel. Chinese Journal of Physics. 2022; 77():350–365, DOI: 10.1016/j.cjph.2021.10.049.
3. M. Oubella, M. Feddaoui, and R. Mir. Numerical study of heat and mass transfer during evaporation of a thin liquid film. Thermal Science. 2015; 19(5):1805–1819, DOI: 10.2298/TSCI130128145O.
4. M. M. Ikram, G. Saha, and S. C. Saha. Conjugate forced convection transient flow and heat transfer analysis in a hexagonal, partitioned, air filled cavity with dynamic modulator. International. Journal of Heat and Mass Transfer. 2021; 167():1-18, DOI: 10.1016/j.ijheatmasstransfer.2020.120786.
5. V. H. Fanambinantsoa, F. d'Assise Rakotomanga, and M. A. Randriazanamparany. Numerical study of forced convection in a horizontal rectangular channel with a sinusoidal protuberance. Afrique Science. 2016; 12(6):353–364. French
6. O. Oulaid, B. Benhamou, and N. Galanis. Effect of variability in thermo-physical properties on paired heat and mass transfer in a vertical channel. 14th International Thermal Days. 2009.
7. W. Ghrissi, G. Promis, T. Langlet et al. Study of the influence of input parameters in an air channel on mass and heat transfer phenomena within a wall saturated with water : application to the renovation of old wet buildings. Journal of Building Performance Simulation. 2022; 15(1):81–96, DOI:10.1080/19401493.2021.1994651.

8. N. Boukadida and S. Ben Nasrallah. Mass and heat transfer during water evaporation in laminar flow inside a rectangular channel - Validity of heat and mass transfer analogy. International Journal of Thermal Science. 2001; 40(1):67–81, DOI:10.1016/S1290-0729(00)01181-9.
9. Y. Du, S. Wang, D. Li et al. Effect of evaporation rate for the heat and mass transfer of the laminar liquid falling film in still air. Frontiers in Energy Research. 2022; ():1–9, DOI:10.3389/fenrg.2022.899023.
10. L. Merouani *et al.* Numerical study of film condensation by mixed convection in a vertical channel. 13th International Thermal Days, 2007.
11. H. El Baamrani, L. Bammou, A. Aharoune et al. Volume of Fluid (VOF) Modeling of Liquid Film Evaporation in Mixed Convection Flow through a Vertical Channel. Mathematical Problems in Engineering.2021;() : DOI:10.1155/2021/9934593.
12. O. Mechergui. Numerical study of mass and heat transfer in natural convection in a channel: influence of wall shape. Thesis; 2017, Université de Perpignan via Domita.
13. N. Lefi and N. Boukadida. Coupled heat and mass transfer in unsteady evaporation of liquids. Revue des Energies Renouvelables CISM'08 Oum El Bouaghi. 2008;():217–225.
14. D. Helel and N. Boukadida. Heat and mass transfer in an unsaturated porous medium subjected to laminar forced convection. 13th International Thermal Days, 2007.
15. M. A. Kassim and S. Harmand. Combined heat and mass transfer with phase change in a vertical channel. Computational Thermal Sciences: An International Journal. 2010; 2(4):299–310, DOI:10.1615/ComputThermalScien.v2.i4.10.
16. S. Turki, H. Abbassi, and S. Ben Nasrallah. Two-dimensional laminar fluid flow and heat transfer in a channel with a built-in heated square cylinder. International Journal of Thermal Science. 2003; 42():1105–1113, DOI:10.1016/S1290-0729(03)00091-7.
17. S. Zermane, S. Boudebous, and N. Boulkroune. Numerical study of laminar mixed convection in ventilated cavities. Sci. Technol. 2005; 23():34–44.
18. D. M. Diallo. Mathematical modelling and numerical simulation of hydrodynamics: the case of flooding downstream of the Diama dam. Thesis; 2010, Université de Franche-Comté, France.
19. M. Feddaoui, A. Mir, and E. Belahmidi. Cocurrent turbulent mixed convection heat and mass transfer in falling film of water inside a vertical heated tube. International Journal of Heat and Mass Transfer. 2003; 46(18):3497–3509, DOI:10.1016/S0017-9310(03)00129-7.
20. E. R. . Eckert and R. . Drake Jr. Analysis of heat and mass transfer. New York : McGraw-Hill, 1972.
21. J.-F. Sacadura, Transferts thermiques : Initiation et approfondissement. Paris, 2015.
22. O. Oulaid. Transfert couplé de chaleur et de masse par convection mixte avec changement de phase dans un canal. Thesis; 2010, Université de Sherbrooke.

******